EUROPEAN ORGANIZATION FOR NUCLEAR RESEARCH

CERN-SL-99-072 AP
CLIC Note 421

Thermal and acoustic effects in CLIC beam absorbers

J.B. Jeanneret and E. Wildner

Abstract

We study thermal and acoustic effects in the beam absorbers of CLIC. While solid dumps and water at ordinary temperature must be ruled out, we propose to make a dump of water working at 4 °C, where the thermal elongation vanishes. This solution might solve the problem of excessive acoustic emission in the dumps which would otherwise prevent the collision of the beams.

Geneva, Switzerland
October 1999

1 Introduction

This study was triggered by Olivier Napoly [1] who pointed out the potential difficulties to control at nanometric scale a beam line whose magnetic elements could experience vibrations generated by the dumps. In this note we consider heat deposition issues before looking further at the associated acoustic waves. Some numbers are quite impressive with CLIC beams and severe limitations appear as for the choice of dump materials. We first consider solid dumps, thermally (Sections 2.3 and 3) and acoustically (Section 4) and show that both melting and stress limits are largely exceeded. We estimate the tolerance of the CLIC beams to vibrations of the quadrupoles in the chromatic correction section (CCS) and in the final doublet (FD) and compare them to the acoustic power emitted by the dumps. We show that, expressed in terms of power, the emission of acoustic waves exceeds the tolerances by several orders of magnitude (Section 4.3). While a dump made of water at ordinary temperature is acceptable thermally, it is not as good as solid dumps acoustically (Section 5). We thus propose to make a dump of water working near the temperature $T_\circ = 4$ °C, where the thermal expansion becomes negligible. This promising solution offers an attenuation by several orders of magnitude of the emitted acoustic power when compared to either solid materials or water at ordinary temperature (Section 6).

2 Basic parameters

2.1 Dump materials

As a first approach to the problem, we considered a dump made of a single block of material which contains all of the energy of the impacting electrons. This simplification will be commented later. As for the choice of materials, we simply considered a low-Z, a medium-Z and a large-Z material. Graphite has very interesting mechanical and thermal properties, copper has a good heat conductivity and tungsten is the best high-Z material mechanically and thermally. This choice is by far not exhaustive but is adequate to draw a few clear conclusions. Some basic data are presented in Table 1 for a few materials. No attempt was made to consider detailed dependence with density or temperature. We just verified the absence of drastic variations which would falsify our simple calculations. Our main sources of information were references [2] and [3]. We got some informations about graphite thanks to Murray Ross [5].

2.2 Electromagnetic shower

The absorption of electrons, positrons and photons (all called particles below) in a massive object can be described to an adequate precision with a single parameter called the radiation length named here L_R which depends almost only on the

Table 1: Thermal and mechanical parameters for graphite (C), copper (Cu) and tungsten (W), together with notional electomagnetic shower parameters. For all these data, variations of the order of $\pm 20\%$ must be expected, depending on fabrication processes, density and other parameters. The average specific heat $\overline{c}_v$ is an estimate between room temperature T_o and melting point T_m . The quantity $\Delta Q_m = \overline{c}_v \Delta T_m$ is the melting heat with $\Delta T_m = T_m - T_o$. The thermal expansion is defined at room temperature. Its variation with T is not significant (compare room temperature values to $\alpha_C(2000^\circ) = 5 \times 10^{-6}$, $\alpha_W(2000^\circ) = 5.5\ 10^{-6}$). The critical internal stress is estimated for a lifetime of 10^6 cycles and is a notional average over many materials. For a specific material, variations of the order $\pm 60\%$ must be expected. As for electromagnetic showers, we made quite crude estimates, restricting the volume of the shower to its dense central core, considering a length of ten radiation lengths and a diameter of two radiation lengths. We used the surface and the volume of the corresponding parallelipiped as an effective surface and volume of the shower. We considered as well the density of energy deposition to be constant in this volume, as explained in the text.

Parameter	Unit	C	Cu	W
Density ρ	[g cm^{-3}]	2	8.96	19.3
Specific heat $\overline{c}_v$	[J cm$^{-3}(^\circ)^{-1}$]	1.6	3.4	3.5
Melting temperature T_m	[$^\circ$]	3500	1100	3400
Melting heat ΔQ_m	[Jcm^{-3}]	5.6×10^3	3.7×10^3	1.2×10^4
Heat conductivity w_q	[J cm$^{-1}(^\circ)^{-1}$s^{-1}]	0.24	3.9	2.0
Thermal elongation α	[$(^\circ)^{-1}$]	3×10^{-6}	2×10^{-5}	4×10^{-6}
Elastic modulus Y	[Pa]	5.4×10^9	1.25×10^{11}	3.9×10^{11}
Critical Internal stress σ_c	[Pa]	4×10^8	4×10^8	4×10^8
Radiation length L_R	[cm]	19	1.4	0.35
E-M Shower :				
effective length $L_{sh} = 10 L_R$	[cm]	190	14	3.5
effective diametre $2L_R$	[cm]	38	2.8	0.7
effective surface $S_{sh} = 80 L_R^2$	[cm^2]	2.9×10^4	160	9.8
effective volume $V_{sh} = 40 L_R^3$	[cm^3]	2.7×10^5	110	1.7

atomic number Z and on the density of the material ρ. The radiation length is the electromagnetic mean free path for ultrarelativistic particles. The final state after one interaction is often made of two particles, which interact again after L_R in average. The process is continued and multiplies the number of particles until their energy is too small to allow further interactions . This statistical process, called "electromagnetic shower", increases the energy deposition for increasing depth z of traversed material . The process reaches a broad maximum between around $z \approx 10\ L_R$ and dies slowly after $z \sim 20 L_R$ [3]. The energy deposition in the medium occurs by the ionisation induced by the charged particles. Its local density is proportional to the local density of tracks. In the transverse $x-y$ plane and near its longitudinal maximum, the shower has an approximately gaussian transverse profile with an r.m.s of $\approx L_R$. The effective volume of the shower which is related to the central density of the shower is therefore proportional to L_R^3, introducing strong variations of the thermal behaviour between different materials (see Table 1).

2.3 Energy and power of collision products

Using the present set of beam parameters of the CLIC beams[1] ($N_b = 4\ 10^9$ particles per bunch separated by $\tau_b = 0.67$ ns, 150 bunches per train, $f = 75$ trains per second, and finally a beam energy of 1.5 TeV) the energy per beam train and the average steady power per beam to be dumped are those given in Table 2. Following D. Schulte [4], we split the total energy and power somewhat arbitrarily in three categories, depending on what happens to colliding particles at the crossing point. The categories are

Beam out This contains the particles which do not 'visibly' interact.

Beamstrahlung The beamstrahlung photons at the collision point.

e^+e^- pairs The e^+e^- pairs produced coherently at the collision point.

This is a very approximative approach. The electrons in the final state after beamstrahlung do not appear explicitly. Neither the location of the dumps nor the size of the spot of impact at the entrance of the dumps are known at present. It might be for example that the first two categories pile up. It is also not known at present how we can expect to play with these collision products to spray them on large dump areas. The particles of each category are considered as forming pencil beams, each category being dumped on a separate device.

[1] During the course of this study, the CLIC parameters were slightly modified, but not so much as to modify substantially enough our results and even less our conclusions. We therefore did not update our numerical calculations.

Table 2: Energy of an beam train (upper part) and steady beam power (lower part. The first column contains the total energy or power of one beam. These quantities are split in three kinds of collision products in the trailing columns, see text.

E_{train} [kJ]	$E_{\mathrm{beam,out}}$ [kJ]	$E_{\mathrm{beamstrahlung}}$ [kJ]	$E_{e^+e^-}$ [kJ]
143.3	85	53	5.3
P_{train} [MW]	$P_{\mathrm{beam,out}}$ [MW]	$P_{\mathrm{beamstrahlung}}$ [MW]	$P_{e^+e^-}$ [MW]
10.8	6.4	4	0.4

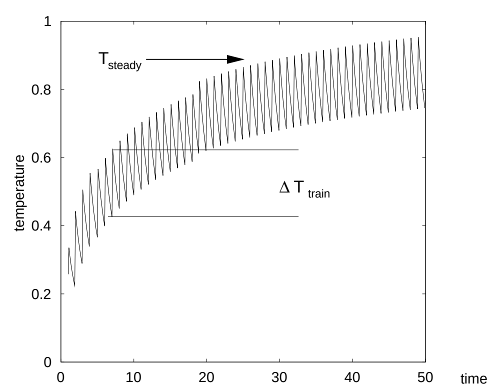

Figure 1: The time dependence of temperature in the dump illustrated. Units are arbitrary. The small steps correspond to the bunch train structure. The slow rise happens at start-up and is followed by a steady state.

3 Temperature rise of dump elements

Temperature rise must be considered in two different ways, illustrated in Figure 1. The deposition of heat of a bunch train, which lasts 100 ns, is adiabatic (see Section 4.1 about that condition). The temperature is thus increasing by a fast step given by the density of energy deposition ϵ in the core of the shower divided by the specific heat $\overline{c}_v$, or

$$\Delta T_{\text{train}} = \epsilon/\overline{c}_v = \frac{E}{\overline{c}_v V_{\text{shower}}} \tag{1}$$

where E is the energy per train of one of the kinds of collision products, see Table 2. The quantity ΔT_{train} is given in Table 3 together with a melting number $m_{\text{train}} = \epsilon/\Delta Q_{\text{melting}}$, this last quantity being an indication of which material is usable as a dump.

The average equilibrium temperature at the core of the shower is obtained by solving the heat equation for a position-dependent power deposition in a much simplified way. We consider a linear transverse decay of the temperature (illustrated in Figure 2), related to our simplified constant power map inside the core of the shower. The length of the shower along the Z axis is ~ 5 times larger than its transverse width, we therefore neglect the longitudinal flow of heat. For a given $T_{\text{steady}} = T_{\text{max}}$ at the crest of the shower (see Figure 2), the integrated flow of power is

$$P_{\text{out}} = w_q \frac{\partial T}{\partial x} S_{sh} = w_q \frac{T_{\text{max}}}{L_R} S_{sh}. \tag{2}$$

Definition and constants are given in Table 1. The maximum temperature $T_{\text{max}} = T_{\text{melting}}$ is obtained by the substitution $P_{out} = P_{in}$ in (2) , with P_{in} taken from Table 2. We define a steady melting number with $m_{\text{steady}} = T_{\text{max}}/\Delta T_m$, with the melting temperature ΔT_m taken in Table 2. The results are given in Table 4.

Immediate conclusions can be drawn by contemplating Table 4. No solid material can be envisaged for the 'Beam out' and the 'Beamstrahlung' dumps. As for dumping e^+e^- pairs, graphite and copper might be envisaged if routine operation of a device near 1000° is doable. The inspection of Table 3 indicates that the impact of even a single train excludes the use of tungsten.

The heat might potentially be evacuated out of the dumps with water (or another liquid). But the segmentation of the flow of water shall be of the order of $\sim 0.1 L_R$, in order to satisfy the condition $m_{\text{steady}} < 1$. The robustness of such a dump is very questionable, and we believe that this option shall not be considered a priori. We prefer to evaluate first a dump made of liquid. This is discussed in Section 5 and 6.

Table 3: Temperature rise per train $\Delta T_{\mathrm{train}}$ of the different dumps (upper part) and the corresponding melting number m_{train} (lower part) for different materials. See text for the calculations.

Material	Beam out	Beamstrahlung	e^+e^-
$\Delta T_{\mathrm{train}}$			
C	0.20°	0.12°	0.01°
Cu	230°	140°	14°
W	14000°	9000°	900°
m_{train}			
C	$6\ 10^{-5}$	$4\ 10^{-5}$	$4\ 10^{-6}$
Cu	0.2	0.13	0.01
W	4.2	2.6	0.26

Table 4: Melting number m_{steady} of the different dumps for different materials. See text for the calculations.

Material	Beam out	Beamstrahlung	e^+e^-
m_{steady}			
C	5.0	3.1	0.31 (1200°)
Cu	13	8	0.8 (900°)
W	33	21	2

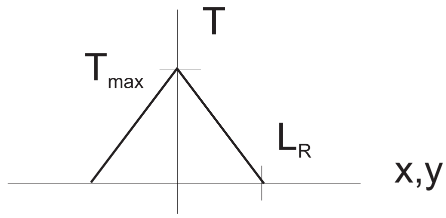

Figure 2: Simplified transverse temperature distribution, used to estimate the the peak steady temperature of the dump block.

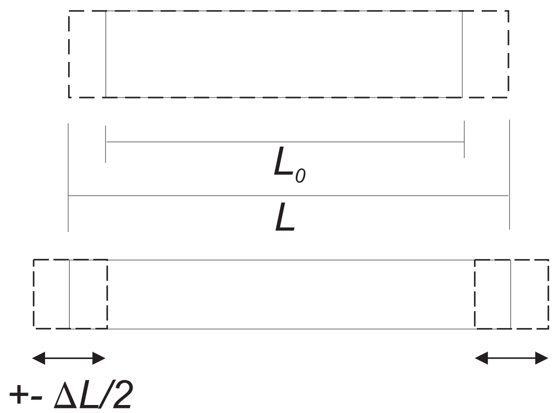

Figure 3: Oscillation induced by adiabatic temperature rise.

4 Acoustic waves

Vibrations, or acoustic waves are produced in matter when heat deposition is sudden enough to prevent heat to propagate substantially in the volume heated and also to prevent elongation with temperature to occur during the time of heat release. The time scale related to adiabatic release of heat will be discussed in Section 4.1. Let us first consider a simple 1D-model (Figure 3). A thin bar of matter of length L_0 is heated in an infinitely short time from temperature T_0 to T. By inertia and with the coefficient of elongation α, the bar cannot expand smoothly to its new rest length $L = L_0 + \Delta L = L_0[1 + \alpha(T - T_0)]$ as it would do with slow enough heating. It is therefore still at its initial rest length L_0 while the temperature already increased. The bar is therefore "compressed" by a factor $\Delta L/L$, with an internal unit stress σ given by Hooke's law $\Delta L/L = \sigma/Y$, with Y being the Young modulus. But the bar is also free to move. The Hooke law is linear, therefore the bar will oscillate harmonically in the range of length $[L - \Delta L, L + \Delta L]$. In this simple case, the amplitude of the acoustic wave at the end of the bar is $\Delta L/2$.

In a more general case, considering longitudinal pressure plane waves, we obtain a wave equation by considering a thin slice of the former bar of unit transverse surface. With the left and the right side x and $x + \mathrm{dx}$ of the slice moved respectively by $\xi(x)$ and $\xi(x+\mathrm{dx}) = \xi(\mathrm{x}) + \frac{\partial\xi}{\partial \mathrm{x}}\mathrm{dx}$, the Hooke law and the law of inertia of Newton write respectively

$$\frac{\partial\xi}{\partial x} = \frac{\sigma}{Y} \quad \text{and} \quad \rho\frac{\partial^2\xi}{\partial t^2} = \frac{\partial\sigma}{\partial x} \tag{3}$$

with ρ the density of the material. Combining the two equations after taking the derivative of Hooke's law, the wave equation writes

$$\frac{\partial^2\xi}{\partial x^2} = \frac{Y}{\rho}\frac{\partial^2\xi}{\partial t^2} \ . \tag{4}$$

The speed of sound is $v_{\text{sound}} = \sqrt{Y/\rho}$ with Y and ρ taken from Table 2. Numerically, considering a block of graphite and using Table 2, we get $v_{\text{sound}} = 1600$ m/s. In a block long by $L = 2$ m, the fundamental mode has the wave length $\lambda_0 = 2L = 4$ m, with the extremities of the block free to oscillate and a central node. The fundamental frequency is therefore $\nu_0 = v_{\text{sound}}/\lambda_0 = 400$ Hz.

4.1 Adiabaticity conditions

With the number derived in the former section, the transient time of propagation of the waves through the dump is $\delta t = L/v_{\text{sound}} \approx 10^{-3}$ s. With a duration of the bunch train $\delta t_{\text{train}} = 10^{-7}$ s, the adiabaticity condition is obviously met.

4.2 Acoustic amplitudes in the shower - the case of e^+e^- pairs

Using the simple formulae of Section 4, a notional value of acoustic amplitude per train is obtained with $\delta l = \alpha\Delta T_{\text{train}} L_{sh}$ and in the steady case $\Delta l = f\alpha\Delta T_{\text{train}} L_{sh}$ with $f = 75$ the number of trains per second. Some numbers are given in Table 5. The numbers for copper and tungsten are given just for reference. An approximate stress number is computed with $n_{\text{stress}} = (Y/\sigma_c)\cdot(\Delta l/L_{sh})$. Numerical results are given in Table 5. It was shown in Section 3 that such dumps would melt anyway. Here we just show that they might break before melting. On the other hand, the graphite dump would survive to acoustic waves in the e^+e^- case.

4.3 Acoustic emission in dumps and absorption in magnets

To evaluate the risk to excite the beams to a dangerous level with acoustic waves emitted by the dumps, a simple approach is to compare the power W_e which is emitted by the dumps to the power W_a needed to bring a quadrupole into oscillation at a critical amplitude beyond which the operation of CLIC is compromised.

A rough estimation of the acoustic power emitted by a dump is obtained by considering isotropic compression only and, as before, also by neglecting

Table 5: Acoustic amplitudes per train (δl) and steady ones (Δl) in the e^+e^- dump. The steady amplitudes are computed as a coherent addition of the train waves and with a quite arbitrary damping time $\tau_{damping} = 1$ s and shall be understood in practice as the integral of a spectral density, see text. The amplitudes δl and Δl are computed over the effective shower length $L_{sh} = 10L_R$, see Table 2. A stress number $n_{stress} > 1$ indicates that the material shall not resist the thermal shock.

Material	δl [nm]	Δl [mm]	$n_{\rm stress}$	$\nu_{\rm exc}$ [Hz]
C	70	5 10−3	$4\ 10^{-5}$	400
Cu	$4\ 10^4$	3	7	$2\ 10^4$
W	$1.2\ 10^5$	9	260	$2\ 10^5$

shear waves (most likely a good approximation, the thermal elongation being an isotropic process in ordinary materials). The energy emitted by a train can be computed as

$$E_e = \frac{3}{2} Y V_{sh} \left(\frac{\delta l}{l}\right)^2 = \frac{3}{2} Y V_{sh} \alpha^2 (\Delta T_{\rm train})^2 \tag{5}$$

which gives for the steady state

$$W_e = f E_e = \frac{3}{2} f Y V_{sh} \alpha^2 (\Delta T_{\rm train})^2 \ . \tag{6}$$

The results, given in Table 6, must be compared to the power needed to excite an oscillation in a magnet. In the absence of a precise design of the magnets of CLIC, we considered a simple object weighting $m = 1000$ kg supported by a steel plate of section $S = 2\ 10^{-3}$ m^2 and height $h = 0.5$ m. This assembly is a harmonic oscillator, at least in the vertical plane (coordinate y with $y = 0$ the rest position of the assembly). The support plays the role of the spring with a linear recoil force $F_{\rm recoil} = S\sigma$ with $\sigma = Y\delta h/h$ the stress in the support and Y the Young modulus. With $\delta h = y$ the elongation of the support and y the corresponding vertical displacement of the quadrupole we write $F_{\rm recoil} = YSy/h = ky$ and thus $k = YS/h$. With yet undefined friction coefficient r and external force F_{ext}, the equation of the motion is

$$\ddot{y} + \frac{r}{m}\dot{y} + \frac{k}{m} y = \ddot{y} + \gamma\dot{y} + cy = \frac{F_{ext}}{m} \ . \tag{7}$$

The proper frequency is $\omega_o = \sqrt{c} = 895$ rad/s or $\nu_o = \omega_o/2\pi = 142$ Hz, with $E = 2 \times 10^{11}$ Pa for steel. In the absence of good data for r, we considered, maybe optimistically, that the oscillator is at the critical damping, i.e. $\gamma = 2\omega_o$, such that the power needed to excite the oscillator to an amplitude δy is

$$W_a = \frac{1}{2}\gamma m\omega_o^2 A^2 = m\omega_o^3(\delta y)^2 \ . \tag{8}$$

The tolerable amplitude of a transverse displacement of the beam shall be close to $A_c = \sigma_\beta/10$ to avoid significant loss of luminosity.

The sensitivity of the colliding beams to the displacement of magnetic elements of the beam has been treated exhaustively by S. Farthouk [8, 9]. A vertical displacement δy of a quadrupole at the local maximum of beta $\beta_{\mathrm{ccs}} = 6 \times 10^5$ m in the chromatic correction section (CCS) induces a displacement at the IP given by

$$\delta y^* = \sqrt{\beta_{ccs}\beta^*}\,\sin(\mu^* - \mu)KL\delta y = 0.13\,\delta y_{ccs} \tag{9}$$

where $\mu^* - \mu = n\pi + \pi/2$, $KL = 0.0167\ \mathrm{m}^{-2}$ and $\beta^* = 10^{-4}$ m [1, 7]. The tolerance of the oscillation of the CCS quadrupoles is therefore $\delta y_{\mathrm{ccs}} = (0.1/0.13)\sigma_y^* = 0.5$nm with $\sigma_y^* = 0.6$ nm [1].

In the final doublet, with a phase advance of 90° between the quadrupoles and the crossing point, a transverse displacement of δy_{fd} of a quadrupole displaces the beam by the same quantity δy_{fd} at the crossing point. The critical amplitude of excitation in the doublet section is therefore fixed by the vertical beam size at the crossing point $\delta y_{\mathrm{fd}} = 0.1\,\sigma_y^* = 0.06$ nm .

The critical power of excitation W_{ccs} and W_{FD} in Table 6 are obtained with the respective replacement $\delta y = \delta y_{\mathrm{ccs}} = 0.5$ nm and $\delta y = \delta y_{\mathrm{FD}} = 0.06$ nm in Formula (8).

4.4 Discussion about acoustic waves

While keeping in view several crude approximations made in order to build the content of Table 6, it nevertheless appears that the beam dump of one beam, which cannot be much distant from the other beam line, has a strong potential of nuisance. For the doublet, the ratio W_a/W_e amounts to about 10^5 and 10^7 when considering the e^+e^- and beam dumps respectively. Even if the self-damping of the graphite (or of another material) is much stronger than our choice $\tau_{\mathrm{damping}} = 1$s and even if the concrete of the tunnels and of the experimental areas is a poor "wave guide", it remains that many orders of magnitude in excess of tolerable acoustic excitation requires careful further studies.

5 A dump made of warm water

With solids likely being unable to do good dumps, liquids must be considered with water being an obvious candidate, at least a priori. Some useful parameters for water are given in Table 5.

Table 6: Steady acoustic power W_e emitted in graphite dumps compared to the power $W_{\rm ccs}$ and $W_{\rm fd}$ needed to excite respectively an oscillation of dangerous amplitude in a quadrupole of the section of chromatic correction and in the quadrupoles of the final doublet (see text).

Dump	$\Delta T_{\rm train}$ [°]	W_e [Watt]
Beam out	0.15	5.7×10^{-2}
Beamstrahlung	0.10	2.2×10^{-2}
e^+e^- pairs	0.01	2.2×10^{-4}
Beam element	A_{crit} [nm]	W_a [Watt]
$W_{\rm ccs}$	0.5	1.7×10^{-7}
$W_{\rm fd}$	0.06	2.5×10^{-9}

5.1 Steady heat flow in water

Contrary to solids, heat conductivity plays little role in liquids at macroscopic scale. The cooling of the dump shall therefore be made by direct water flow. In the main dump and fixing a maximum temperature rise of the water of $\Delta T = 50°$, the flow shall be $\phi = P_{\rm beam,out}/(c_v \Delta T) = 32$ l/s. This flow is small compared to the volume of the dump which must be larger than the volume of the shower $V_{\rm shower} = 1900$ l. It allows laminar flow thus avoiding the potential acoustic problems associated to turbulent flow.

5.2 Acoustic waves in water

The production of acoustic waves with heat is similar in liquids and solids. Liquids do not carry transverse waves, but we did not consider them in solids. Therefore we compute the emitted acoustic power with (6). Replacing the elastic modulus by the inverse of the compressibility κ we get

$$W_e = \frac{3}{2}\frac{f V_{\rm shower}}{\kappa}\left(\frac{\delta l}{l}\right)^2 = \frac{3}{2}\frac{f V_{\rm shower}}{\kappa}\alpha_{lin}^2(\Delta T_{\rm train})^2 \ . \tag{10}$$

For the main dump and using the parameters of Table 7 we get $W_{\rm e,water} = 1.0$ W, i.e. twenty times more acoustic power than in the case of graphite (see Table 7).

Table 7: Thermal and mechanical parameters of water, compared to those of graphite (C).

Parameter	Symbol	Unit	H_2O	C
Density	ρ	[g cm^{-3}]	1	2
Specific heat	c_v	[J cm^{-3}(°)$^{-1}$]	4.18	1.6
Thermal elongation	α	[(°)$^{-1}$]	-	3×10^{-6}
Thermal elongation	$\alpha_{lin} = \alpha_V/3$	[(°)$^{-1}$]	130×10^{-6}	-
Elastic modulus	E	[Pa]	-	5.4×10^9
Inversed Compressibility	κ^{-1}	[Pa]	2.3×10^9	-
Radiation length	L_R	[cm]	36	19
E-M Shower :				
effective length	$10L_R$	[cm]	360	190
effective diametre	$2L_R$	[cm]	72	38
effective surface	$80L_R^2$	[cm^2]	1.04×10^5	2.9×10^4
effective volume	$40L_R^3$	[cm^3]	1.9×10^6	2.7×10^5
Temperature step	ΔT_{train}	[°]	0.01	0.15

We can conclude that while the heat transfer in the main dump can quite easily be made with a moderate flow of water, the emission of acoustic waves is too large in a range of temperature around $T = 50$ °C.

6 A dump made of water at $T_o = 4$ °C

Water is a liquid which has the maybe unique property of a density function with temperature $\rho(T)$ which reaches a maximum near $T_o = 4$ °C. This property can also be expressed by saying that the thermal expansion is zero at T_o by using the relation $d\rho/\rho = -dV/V = -\alpha_V(T)$. We therefore explore the possibility of using this unique feature to suppress the production of acoustic waves. Our basic argument is that in the absence of thermal expansivity, no compression occurs after an adiabatic deposition of heat, thus preventing the relaxation which is at the origin of the acoustic waves. A second argument which will be quantified below is related to the small step of temperature ΔT_{train} which occurs at the time of impact of a bunch train on the dump. This value shall of course be small enough to avoid a significant change of the value of the thermal expansivity.

We now evaluate which temperature range must be considered to get an adequate suppression factor. With thermal expansivity data from [2], we fit to good precision a linear temperature dependence of the volumetric thermal expansivity around T_o as

$$\alpha_v(T) = \alpha_{o,v} \cdot (T - T_o) \tag{11}$$

with $\alpha_{o,v} = 16.05 \times 10^{-6}$. To simplify the comparison with solid materials, we define a linear thermal expansivity $\alpha(T) = \alpha_v(T)/3$ or

$$\alpha(T) = \alpha_o(T - T_o) = 5.35 \times 10^{-6}(T - T_o) \ . \tag{12}$$

With (12), the elongation between the temperatures T_1 and T_2 is

$$\frac{\Delta l}{l_1} = \int_{T_1}^{T_2} \alpha(T)dT = \alpha_o \int_{T_1}^{T_2} (T - T_o)dt = \frac{\alpha_o}{2}\left[T_2^2 - T_1^2 - 2T_o(T_2 - T_1)\right] \tag{13}$$

with l_1 the linear size of the heated sample at T_1. The function (13) is shown in Figure 4 for $T_1 = T_o$ and $T_2 = T$ together with published dV/V data.

To evaluate the emitted acoustic power, we substitute $T_1 = T$ and $T_2 = T + \Delta T_{\text{train}}$ in (13) with ΔT_{train} taken from Table 7 and get

$$\frac{\Delta l}{l} = \alpha_o \left[(T - T_o)\Delta T_{train} + \frac{1}{2}\Delta T_{train}^2\right] \ . \tag{14}$$

We finally compute the acoustic power with Formula (10) in which dl/l is replaced by its expression in Formula (14) with the result

$$W_e = \frac{3fV_{shower}\alpha_o^2}{2\kappa}\left[(T - T_o)\Delta T_{train} + \frac{1}{2}\Delta T_{train}^2\right]^2 \ . \tag{15}$$

The numerical results are given in Table 8. In a crude approach of these numbers, if

$$|T - T_o| < 0.2^\circ \quad \text{then} \quad \mathrm{W_e} < 5\ 10^{-5}\ \text{Watt} \ . \tag{16}$$

This limit is still a factor hundred above the tolerable power in the CCS. But we shall remember that we considered a quite arbitrary damping time τ_{damping} of the dump assembly. By proper acoustic insulation in the dump, a better damping is likely to be achievable. As well, the power W_e is the integral of a spectrum $dW_e/d\omega$ which spreads approximately a low and a high frequenecy fixed respectively by the length and the width of the shower, i.e. $\lambda_{\max} \approx 20L_R = 7.2$ m and $\lambda_{\min} \approx 4L_R = 1.4$ m. Using $\nu = v_s/\lambda$ with the speed of sound in water $v_s = 1/(\rho\kappa)^{1/2} = 1500$ m/s, we get

$$\nu_{\min} \approx 200 \text{ Hz} \qquad \nu_{\max} \approx 1000 \text{ Hz} \tag{17}$$

The quadrupoles with a proper acoustic frequency estimated in Section 4.3 to be near $\nu \approx 140$ Hz will not absorb all of the emitted spectrum. We therefore conclude that if the temperature can be confined precisely enough around $T_o = 4$ °C in its active part a dump of water would solve the problem of the emission of acoustic vibrations. As for the even lower tolerance in the FD area, we will see in Section 7 that the dump shall be located quite far from there. This might solve or at least help to solve the problem, but this point requires further attention.

We finally rapidly evaluate the conditions needed to satisfy (16). We assume a flow a water moving in the transverse plane of the shower (see Figure 5). The temperature at the centre of the shower shall stay inside a range $[T_o - \delta_1 T, T_o + \delta_1 T]$. We express the gradient of temperature integrated across the transverse size of the shower with $2\delta_2 T$. Combining these two conditions in order to satisfy approximately the condition (16), the allowed temperature excursion at the effective edge of the shower shall be

$$\delta_1 T + \delta_2 T < 0.3^\circ \ . \tag{18}$$

With a guess value $\delta_1 T = 0.1^\circ$ it follows $\delta_2 T = 0.2^\circ$. The flux of water shall be

$$\phi = \frac{P_{\text{beam,out}}}{4.18 \ 10^3 \times 2\delta_2 T} = 3.8 \ 10^3 \ \text{l/s} = 3.8 \ \text{m}^3/\text{s} \ . \tag{19}$$

With effective shower width $h_{\text{eff}} = 2L_R = 0.72$ m and depth $d_{\text{eff}} = 10L_R = 3.6$ m, the speed of the water is $v_{\text{water}} = \phi/(h_{\text{eff}} d_{\text{eff}}) \approx 1.5$ m/s. With such section and flow, the regime shall not be turbulent.

The volume of the installation, the installed power and its regulation certainly require more careful studies.

7 Dump location

The crossing angle of the CLIC beams shall be of the order of $\alpha_c = 10$ mrad [1]. The distance between the beams thus grows linearly with the distance to the IP in the absence of strong bending dipoles, which would induce excessive synchrotron radiation levels (while beamstrahlung photons cannot be bent anyway). With a half size of the dump $\Delta x > 2$ m, the dump shall therefore be distant by at least $\Delta s > \Delta_x/\alpha_c = 100$ m. The entrance window of the main dump must sustain the passage of $\dot{n}_e = 4.15 \times 10^{13}$ electrons/s. In a sheet of stainless steel of thickness $t = 1$ mm, the power deposition would be

$$P = \dot{n}_e \frac{dE}{dx} t = 7.6 \ \text{Watt} \tag{20}$$

with $dE/dx = 11.6\text{MeV/cm} = 1.85 \ 10^{-12}$ J/cm. A power $P = 7.6$ Watt is a small number, provided that the beam spot size S in the window is not too small. If $S^{1/2} = 0.5$ cm, the dump must be located at least at $\Delta s > S^{1/2}/\sigma_v^* = 1000$ m with $\sigma_v^* = 5 \ 10^{-6}$ rad the beam divergence at the IP and in the absence of quadrupole in the dump line. For a proton dump, C. Hauviller gave a limit of 10^{13} protons mm^{-2} and proposed a titanium window [10]. With an FD section ending at 20 meters from the IP and a main dump located at > 500 meters,

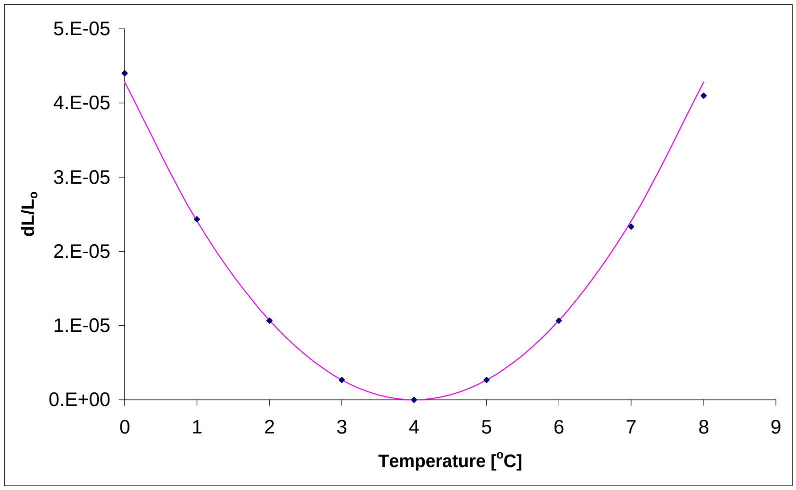

Figure 4: thermal expansion of water around $T_o = 4$ °C. The quantity displayed as a function of the temperature is the quantity $(1/3)(\Delta V/V_o) = (\alpha_o/2)(T - T_o)^2$, see text. The data points are the published values [2] for $\Delta V/V_o$ divided by 3.

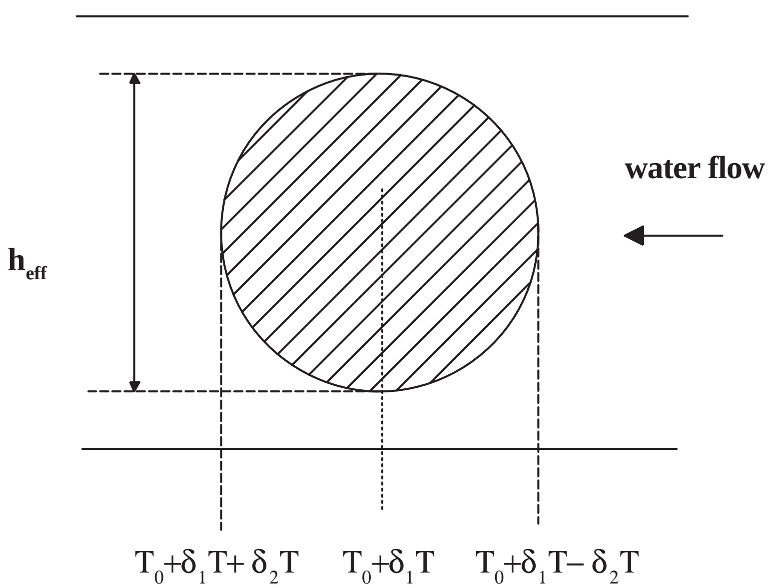

Figure 5: Schematic transverse view of the electron shower in the water flow, see text for notation.

Table 8: Steady acoustic power W_e emitted in water at $T = 4$ °C, compared to water near $T = 50$ °C, to graphite and to the power W_{ccs} and W_{fd} needed to excite respectively an oscillation of dangerous amplitude in a quadrupole of the section of chromatic correction and in the quadrupoles of the final doublet (see text).

Case	$T - T_o$ [°]	W_e [Watt]
Graphite -	-	5.7×10^{-2}
Water near $T_o = 50$ °	-	1.0
Water near $T_o = 4$ °	0.0	3.5×10^{-08}
	0.1	1.6×10^{-05}
	0.2	5.9×10^{-05}
	0.3	1.3×10^{-04}
	0.4	2.3×10^{-04}
	0.5	3.6×10^{-04}
	0.6	5.2×10^{-04}
	0.7	7.0×10^{-04}
	0.8	9.1×10^{-03}
	0.9	1.2×10^{-03}
	1.0	1.4×10^{-03}
Beam element	A_{crit} [nm]	W_a [Watt]
CCS	0.5	1.7×10^{-7}
FD	0.06	2.5×10^{-9}

it can be hoped that distance would help to attenuate the acoustic waves down to the tolerance of the FD quadrupoles, but this point need further work. It shall also be verified with more detailed simulations that the power density in the early part of the shower where it is still narrow is not excessive, thermically and acoustically.

Acknowledgements

The authors wish to thank G. Guignard, S. Fartoukh, C. Hauviller, J. Letry, O. Napoly, D. Schulte and F. Zimmermann for help or advice.

References

[1] O. Napoly , CLIC Note 414, CERN-SL-99-054 AP, DAPNIA/SEA-99-08, 1999.

[2] Handbook of Chemistry and Physics, CRC Press, Cleveland, 55th edition, 1974.

[3] Review of Particle Properties, The European Physical Journal,**3**,1, 1998.

[4] D. Schulte, PAC 99 paper and PS Report PS-1999-017 (LP), CLIC-Note 391, 1999.

[5] Murray Ross, private communication, September 1999.

[6] J.B. Jeanneret , CERN SL/91-39(EA), LHC Note167, 1991.

[7] F. Zimmermann , Private communication, September 1999.

[8] S. Fartoukh, Ph.D thesis, CEA/DAPNIA/SEA-97-02T, Saclay, 1997.

[9] S. Fartoukh and O. Napoly, EPAC98, Stockholm, June 1998.

[10] C. Hauviller, CERN ISR-GE/79-18, PAC San Francisco, 1979.